

Supporting Information

Theoretical study of the adsorption of the butanol isomers in H-ZSM-5

Cuong M. Nguyen, Marie-Fran oise Reyniers*, Guy B. Marin

Laboratory for Chemical Technology, Ghent University, Krijgslaan 281 S5, B-9000 Gent,
Belgium.

*: Corresponding author

Tel: +32 (0) 9 264 4516. Fax: +32 (0) 9 264 4999. E-mail: MarieFrancoise.Reyniers@ugent.be

Contents

Geometrical illustrations of 1-butanol, 2-butanol and t-butanol adsorbed in silicalite and H-ZSM-5 are given. Performance of pbcDFT + D vs. pbc[DFT-D] with respect to geometries, adsorption energies and vibrational frequencies of adsorbed complexes of all the four butanols is detailed. Also, geometrical parameters and physisorption energies of the four butanols physisorbed over the BAS O_aAl[O_bH_z] are presented.

Note: XYZ coordinates of stationary points studied in this work could be obtained from the authors.

S.1. Geometrical Illustrations of butanol isomers (BuOHs) Physisorbed in Silicalite

Figure S.1.1. Physisorption of t-BuOH in silicalite

Figure S.1.2. Physisorption of 2-BuOH in silicalite

Figure S.1.3. Physisorption of 1-BuOH in silicalite

S.2. Geometrical Illustrations of BuOHs Physisorbed over the BAS O_bAl[O_aH_z] of H-ZSM-5

Figure S.2.1. Physisorption of t-BuOH in H-ZSM-5

Figure S.2.2. Physisorption of 2-BuOH in H-ZSM-5

Figure S.2.3. Physisorption of 1-BuOH in H-ZSM-5

S.3. Geometrical Illustration of BuOHs Chemisorbed over the BAS O_bAl[O_aH_z] of H-ZSM-5

Figure S.3.1. Chemisorption of t-BuOH in H-ZSM-5

Figure S.3.2. Chemisorption of 2-BuOH in H-ZSM-5

Figure S.3.3. Chemisorption of 1-BuOH in H-ZSM-5

S.4. Geometrical Parameters and Physisorption Energies of BuOHs Physisorbed over the BAS O_aAl[O_bH_z] of H-ZSM-5

Figure S.4. Representative physisorbed complexes at the BAS O_aAl[O_bH_z]

Table S.4.1. Geometrical parameters

Table S.4.2. Physisorption energies

S.5. Performance of pbcDFT + D vs. pbc[DFT-D]

Table S.5.1. Geometrical parameters of physisorbed silicalite-BuOH complexes

Table S.5.2. Geometrical parameters of physisorbed H-ZSM-5-BuOH complexes

Table S.5.3. Physisorption energies of BuOHs in silicalite

Table S.5.4. Physisorption energies of BuOHs in H-ZSM-5

Table S.5.5. Vibrational frequencies of H-ZSM-5-BuOH physisorbed complexes

Table S.5.6. Geometrical parameters of chemisorbed H-ZSM-5-BuOH complexes

Table S.5.7. Chemisorption energies of BuOHs in H-ZSM-5

Table S.5.8. Vibrational frequencies of H-ZSM-5-BuOH chemisorbed complexes

S.6. Gas phase proton affinities (PA) of butanols computed using Gaussian at the CBS-QB3 level of theory.

Table S.6.1. CBS-QB3 PAs vs. NIST PAs

S.7. Harmonic motions of physisorbed and chemisorbed complexes of butanols in H-ZSM-5

S.7.1. Harmonic motions of physisorbed complexes

S.7.2. Harmonic motions of chemisorbed complexes

References

S.1. Geometrical Illustrations of BuOHs Physisorbed in Silicalite

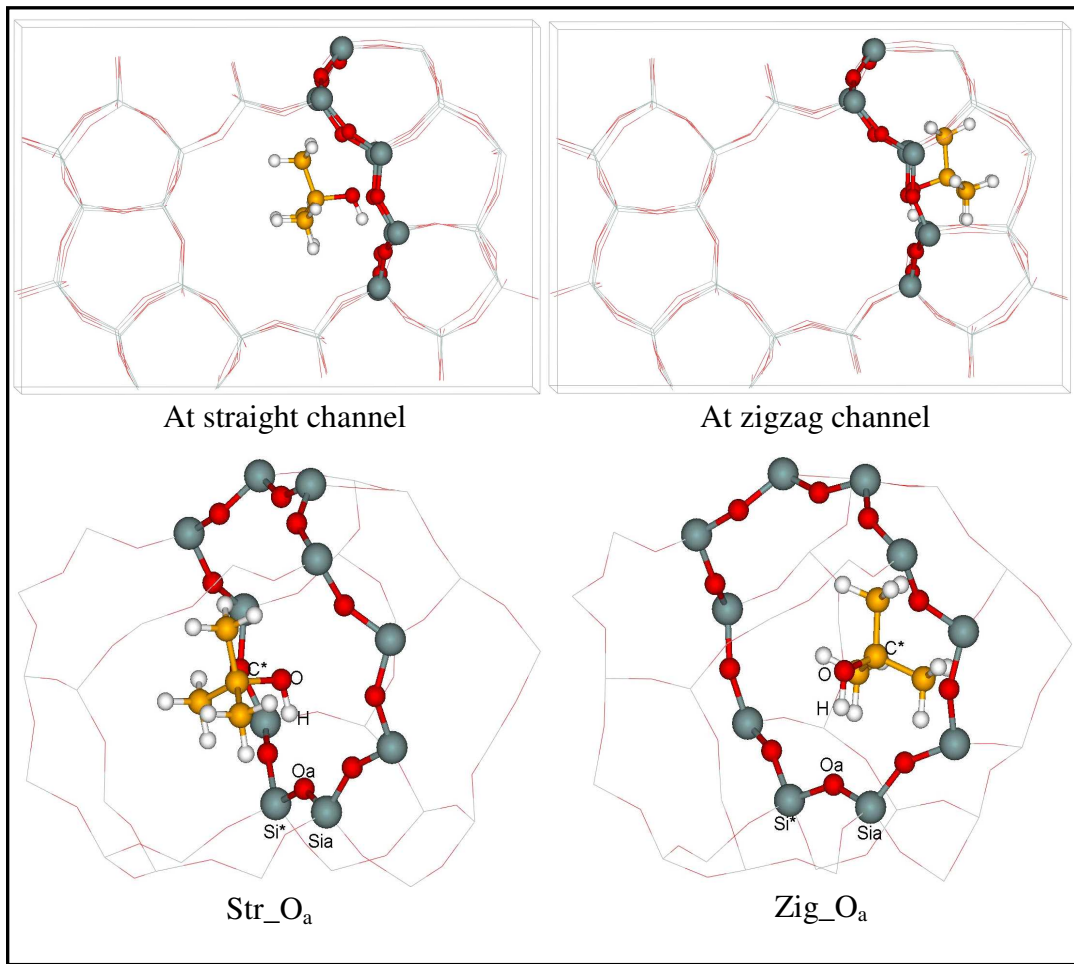


Figure S.1.1. Physisorption of t-BuOH at the *straight* (Str_O_a) and at the *zigzag* channel (Zig_O_a) of silicalite. Highlighted atoms define the 10-T intercrossing ring between the two channels. Si*-O_a-Si_a indicates the T12 bridging position Si12-O24-Si12 for Al substitution at Si* with Si* = Si12, O_a = O24, Si_a = Si12, respectively. The intersection space between the two channels (top pannel) is devided into two parts by the 10-T ring: the left part belongs to the *straight* channel while the right part belongs two the *zigzag* channel. Code colors used: hydrogen (white), oxygen (red), and silicon (grey).

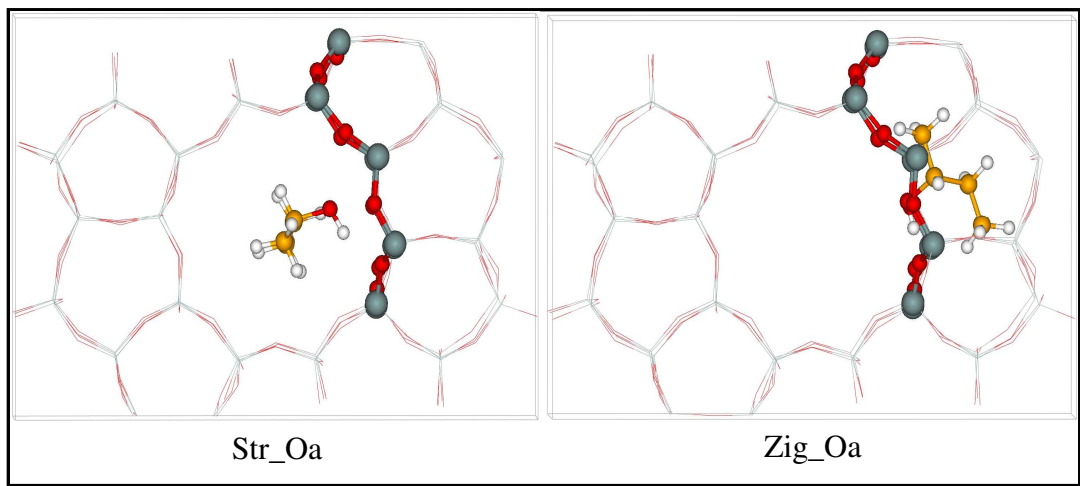


Figure S.1.2. Physisorption of 2-BuOH at the *straight* (Str_O_a) and at the *zigzag* channel (Zig_O_a)

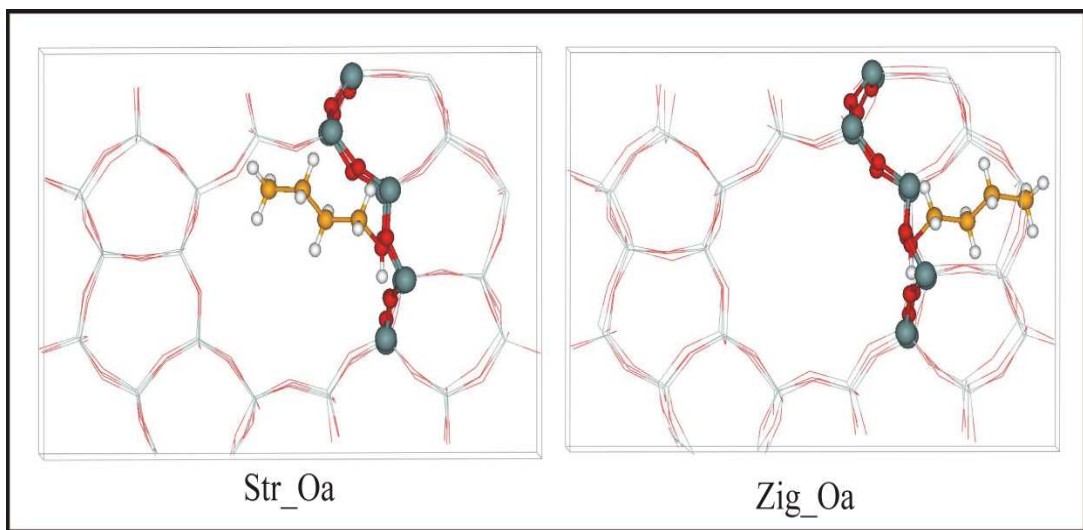


Figure S.1.3. Physisorption of 1-BuOH at the *straight* (Str_O_a) and at the *zigzag* channel (Zig_O_a)

S.2. Geometrical Illustrations of Butanols Physisorbed over the BAS $O_bAl[O_aH_z]$ of H-ZSM-5

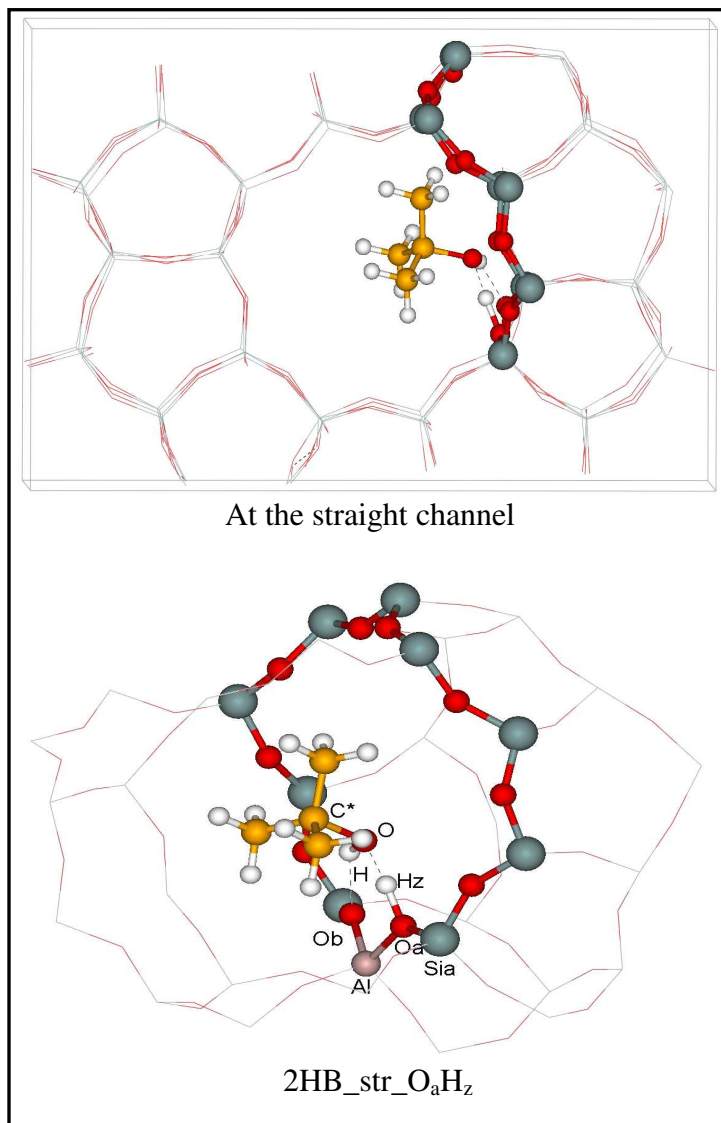


Figure S.2.1. Physisorbed complex $2HB_str_O_aH_z$ of t-BuOH at the *straight* channel of H-ZSM-5. Highlighted atoms define the 10-T intercrossing ring between the two channels. $Si_a = Si12$, $O_a = O24$, $Al = Al12$, and $O_b = O20$, respectively. The intersection space between the two channels (top pannel) is devided into two parts by the 10-T ring: the left part belongs to the *straight* channel while the right part belongs two the *zigzag* channel. Code colors used: oxygen (red), silicon (grey), hydrogen (white), aluminum (pink).

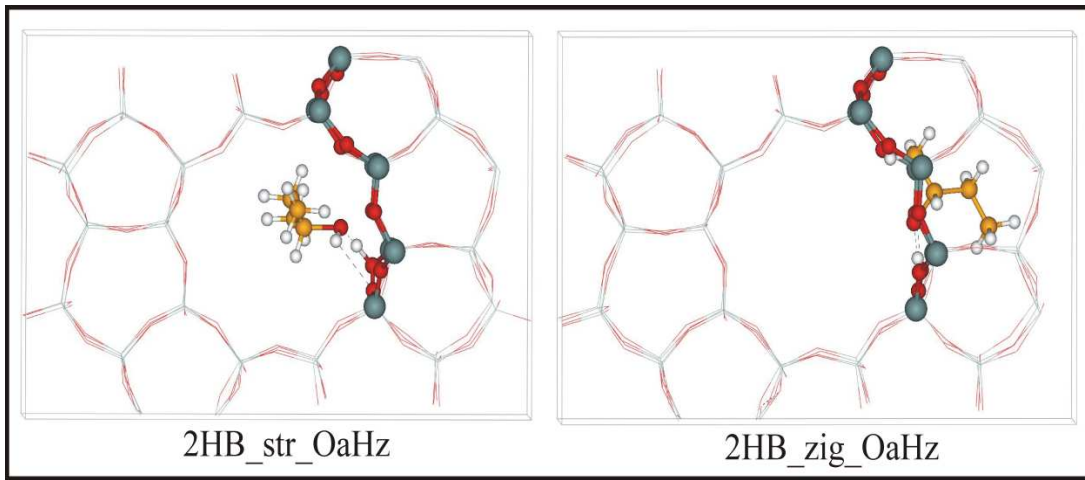


Figure S.2.2. Physisorption of 2-BuOH at the *straight* (2HB_{str}_O_aH_z) and at the *zigzag* (2HB_{zig}_O_aH_z) channel of H-ZSM-5.

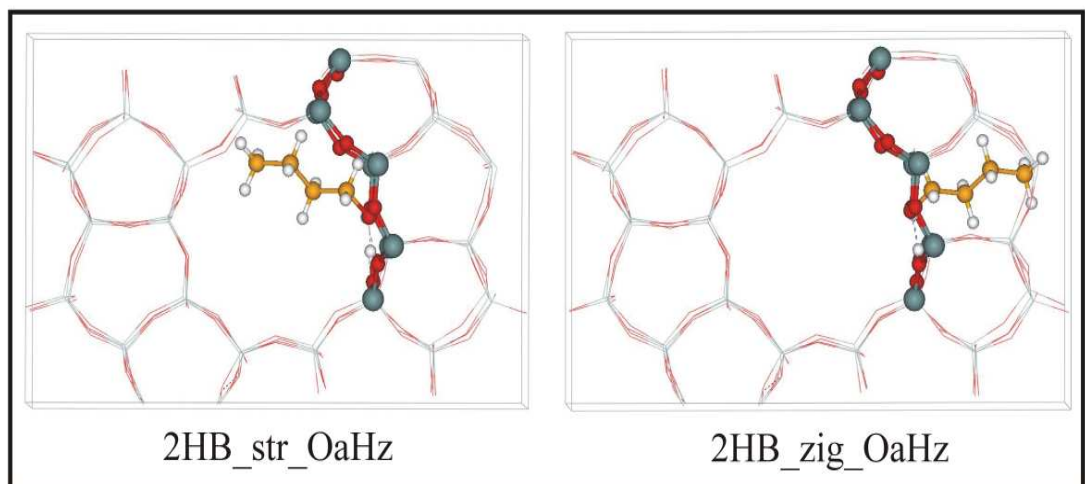


Figure S.2.3. Physisorption of 1-BuOH at the *straight* (2HB_{str}_O_aH_z) and at the *zigzag* (2HB_{zig}_O_aH_z) channel of H-ZSM-5.

S.3. Geometrical Illustrations of Butanols Chemisorbed over the BAS $O_bAl[O_aH_z]$ of H-ZSM-5

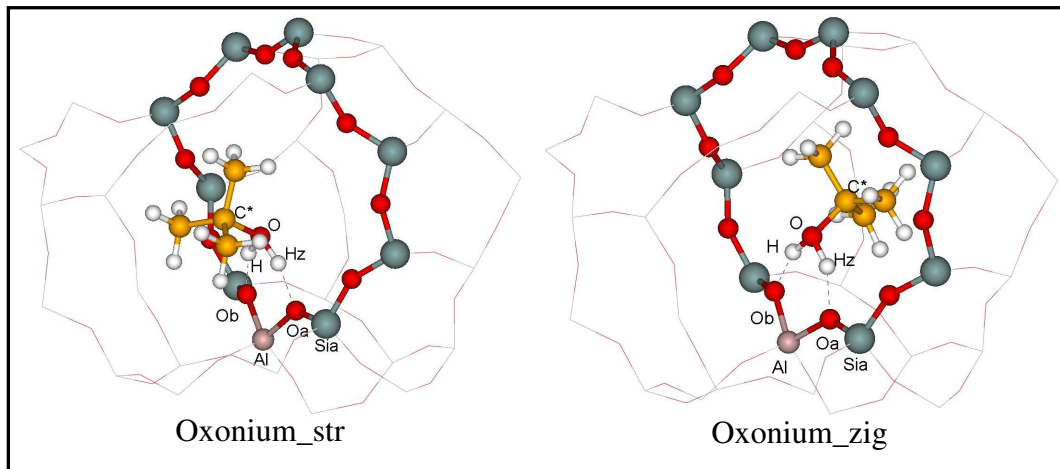


Figure S.3.1. Chemisorption of t-BuOH at the *straight* and *zigzag* channels of H-ZSM-5

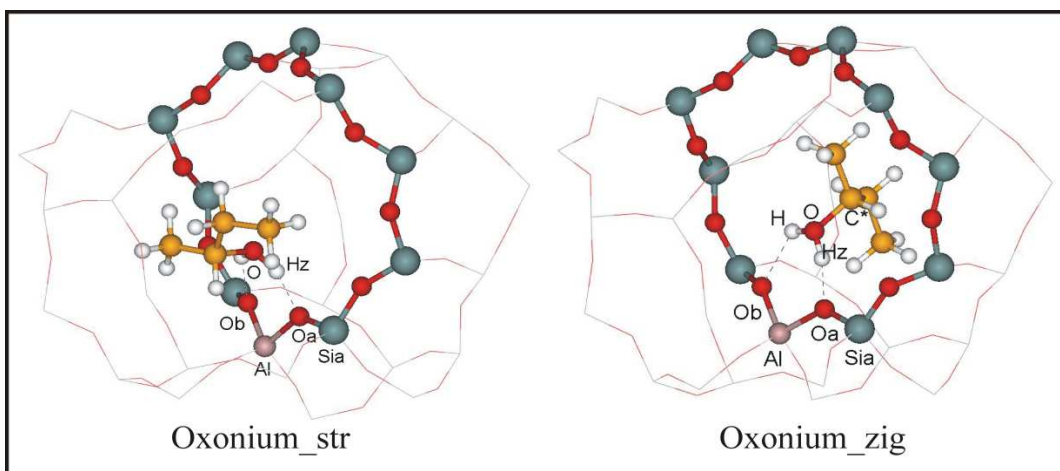


Figure S.3.2. Chemisorption of 2-BuOH at the *straight* and *zigzag* channels of H-ZSM-5

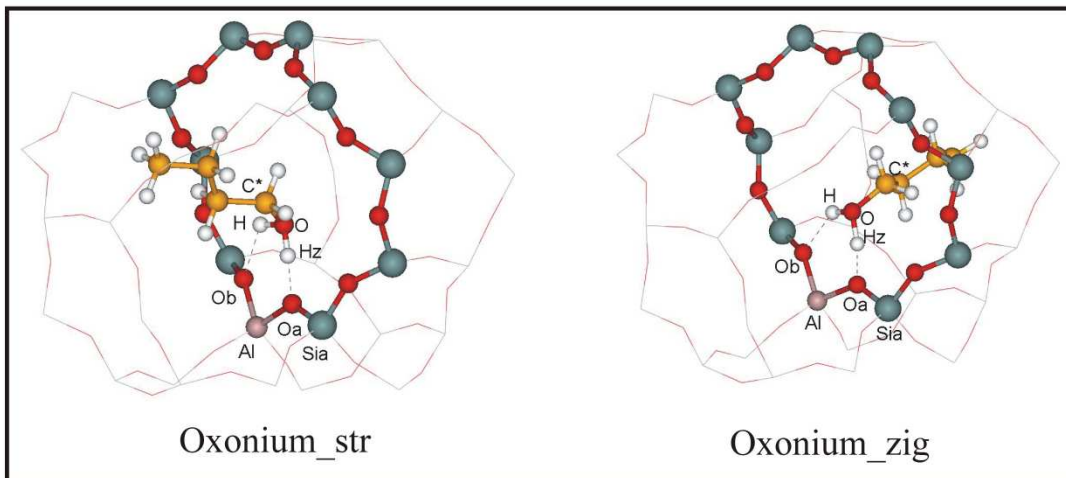


Figure S.3.3. Chemisorption of 1-BuOH at the *straight* and *zigzag* channels of H-ZSM-5

S.4. Geometrical Parameters and Physisorption Energies of BuOHs Physisorbed over the BAS $O_aAl[O_bH_z]$ of H-ZSM-5 obtained using the pbc[DFT-D] approach.

To put in evidence the proton exchange between two adjacent Al12-bound oxygen atoms (O_a and O_b), 2-HB physisorption structures are additionally sampled at the other BAS $O_aAl[O_bH_z]$ with the zeolite proton attached to O_b (Figure S.4). It was observed that the location of the zeolite proton (H_z) at O_a or O_b has insignificant effect on the structural parameters and energetics of the 2-HB physisorbed complexes except those of 2-BuOH (Tables S.4.1 and S.4.2). Over the BAS $O_aAl[O_bH_z]$, 2HB_zig_O_bH_z of 2-BuOH could not be located since all geometrical optimizations starting from physisorbed are relaxed to local minima as the protonated oxonium.

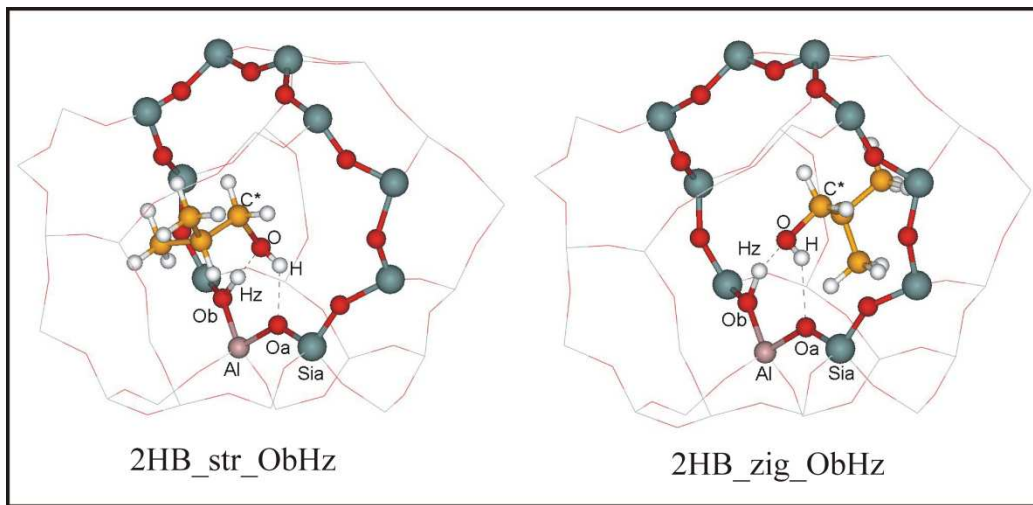


Figure S.4. Representative H-ZSM-5-i-BuOH physisorbed complexes over the BAS $O_aAl[O_bH_z]$: 2HB_{str}-ObHz at the *straight* channel (left panel) and 2HB_{zig}-ObHz at the *zigzag* channel (right panel). Si_a = Si12, O_a = O24, Al = Al12, and O_b = O20, respectively.

Table S.4.1. Geometrical parameters (pm)^a of physisorbed complexes of BuOHs over the BAS $O_aAl[O_bH_z]$ at the *straight* and *zigzag* channels of H-ZSM-5.

	H _z -O _b	H-O	H _z --O	H--O _a
<i>Straight channel</i>	1-BuOH	114.3	99.1	129.9
	i-BuOH	117.5	99.4	125.4
	2-BuOH	120.1	99.2	123.1
	t-BuOH	126.3	99.3	171.8
<i>Zigzag*</i> <i>channel</i>	1-BuOH	117.8	99.1	125.6
	i-BuOH	118.4	99.5	125.0

^aAtom labels and physisorbed complex notations are defined in Figure S.4. *2_HB_zig_ObHz could not be located at the *zigzag* channel for either 2-BuOH or t-BuOH

Table S.4.2. DFT, D, and DFT-D physisorption energies (ΔE_{phys} , kJ mol⁻¹) of BuOHs physisorbed over the BAS O_aAl[O_bH_z] at the *straight* and *zigzag* channels of H-ZSM-5.

		ΔE_{phys}			
		$\Delta E_{\text{DFT-D}}$	ΔE_{DFT}	ΔE_{D}	% ΔE_{D}
<i>Straight channel</i>	1-BuOH	-147	-87	-60	41
	i-BuOH	-146	-83	-63	43
	2-BuOH	-145	-84	-61	42
	t-BuOH	-146	-81	-65	45
<i>Zigzag*</i> <i>channel</i>	1-BuOH	-161	-81	-80	50
	i-BuOH	-150	-53	-97	65

*2_HB_zig_O_bH_z could not be located at the *zigzag* channel for either 2-BuOH or t-BuOH.

S.5. Performance of pbcDFT + D vs. pbc[DFT-D]

Table S.5.1. Geometrical parameters (pm)^a of BuOHs physisorbed at the *straight* and *zigzag* channels of silicalite obtained using pbcDFT and pbc[DFT-D] approaches.

		pbcDFT		pbc[DFT-D]	
		H-O	H---O _a	H-O	H---O _a
<i>Straight channel</i>	1-BuOH	97.5	215.9	97.4	214.1
	i-BuOH	97.6	220.0	97.6	216.2
	2-BuOH	97.4	237.3	97.4	228.5
	t-BuOH	97.6	210.0	97.6	214.4
<i>Zigzag channel</i>	1-BuOH	97.4	228.9	97.4	226.8
	i-BuOH	97.5	248.0	97.5	238.2
	2-BuOH	97.5	207.5	97.6	210.7
	t-BuOH	97.6	210.0	97.6	210.9

^aAtom labels are defined in Figure S.1.1.

Table S.5.2. Geometrical parameters (pm)^a of BuOHs physisorbed at the *straight* and *zigzag* channels of H-ZSM-5 obtained using pbcDFT and pbc[DFT-D] approaches.

	pbcDFT				pbc[DFT-D]			
	H _z -O _a	H-O	H _z --O	H---O _b	H _z -O _a	H-O	H _z --O	H---O _b
Straight channel	1-BuOH	113.5	98.4	130.9	212.6	113.9	98.5	130.4
	i-BuOH	115.9	98.8	128.2	206.0	117.2	99.0	126.3
	2-BuOH	124.3	99.4	119.9	200.7	128.1	99.9	116.6
	t-BuOH	128.5	99.6	115.8	196.7	130.6	99.7	114.2
Zigzag channel	1-BuOH	116.2	99.3	127.8	189.5	117.5	99.3	125.6
	i-BuOH	119.2	99.5	124.9	188.6	119.7	99.5	124.4
	2-BuOH	122.3	99.3	120.0	189.3	126.3	99.4	117.6

^aAtom labels are defined in Figure S.2.1.

Table S.5.3. Physisorption energies (ΔE_{phys} , kJ mol⁻¹) of BuOHs at the *straight* and *zigzag* channels of silicalite obtained using pbcDFT + D and pbc[DFT-D] approaches.

	pbcDFT + D			pbc[DFT-D]		
	$\Delta E_{\text{DFT-D}}$	ΔE_{DFT}	ΔE_{D}	$\Delta E_{\text{DFT-D}}$	ΔE_{DFT}	ΔE_{D}
Straight channel	1-BuOH	-68	-14	-54	-68	-14
	i-BuOH	-68	-13	-55	-66	-10
	2-BuOH	-60	-7	-53	-58	-2
	t-BuOH	-62	-7	-55	-60	1
Zigzag channel	1-BuOH	-83	-7	-76	-79	-4
	i-BuOH	-72	15	-87	-71	20
	2-BuOH	-74	28	-102	-70	33
	t-BuOH	-53	53	-106	-51	59

Table S.5.4. Physisorption energies (ΔE_{phys} , kJ mol⁻¹) of BuOHs at the *straight* and *zigzag* channels of H-ZSM-5 obtained using pbcDFT + D and pbc[DFT-D] approaches.

	pbcDFT + D			pbc[DFT-D]		
	$\Delta E_{\text{DFT-D}}$	ΔE_{DFT}	ΔE_{D}	$\Delta E_{\text{DFT-D}}$	ΔE_{DFT}	ΔE_{D}
<i>Straight channel</i>	1-BuOH	-150	-87	-63	-148	-87
	i-BuOH	-149	-90	-59	-147	-89
	2-BuOH	-146	-83	-63	-144	-81
	t-BuOH	-150	-88	-62	-148	-87
<i>Zigzag*</i> <i>channel</i>	1-BuOH	-161	-80	-81	-160	-76
	i-BuOH	-151	-57	-94	-147	-48
	2-BuOH	-156	-66	-90	-155	-58

*Physisorbed complex of t-BuOH could not be located at the *zigzag* channel

Table S.5.5. Selected harmonic vibration frequencies (cm^{-1})^a for unloaded H-ZSM-5, gas-phase alcohols and most stable physisorbed complexes of BuOHs in H-ZSM-5 obtained using the pbcDFT and pbc[DFT-D] approaches. v: stretching mode; δ : bending mode; $\delta_i(\text{O}_\text{a}\text{H}_\text{z})$ in-plane and $\delta_o(\text{O}_\text{a}\text{H}_\text{z})$ out-of-plane bending mode of the zeolite $\text{O}_\text{a}\text{H}_\text{z}$.

	v(CH)	$\delta(\text{CH})$	$\delta(\text{CH}_3)$	v(OH)	v($\text{O}_\text{a}\text{H}_\text{z}$) ^b	$\delta_i(\text{O}_\text{a}\text{H}_\text{z})$ ^b	$\delta_o(\text{O}_\text{a}\text{H}_\text{z})$
H-ZSM-5					3744	1112	351
1-Butanol							
Gas phase	2905-3061	1437-1471	1358	3765			
2HB_zig_OaHz	2979-3076	1435-1469	1358	3422	1418	1666	1157
t-Butanol							
Gas phase							
2HB_str_OaHz	2987-3085	1423-1455	1385	3400	1410	1738	1207
H-ZSM-5				3737	1110	353	
1-BuOH							
Gas phase	2896-3035	1427-1464	1351	3759			
2HB_zig_OaHz	2964-3067	1427-1460	1350	3425	1392	1669	1171
i-BuOH							
Gas phase	2892-3056	1423-1454	1349	3757			
2HB_str_OaHz	2945-3057	1426-1458	1366	3497	1403	1647	1187
2-BuOH							
Gas phase	2882-3046	1408-1445	1348	3743			
2HB_zig_OaHz	2956-3108	1415-1454	1374	3427	1370	1717	1203
t-BuOH							
Gas phase	2942-3053	1405-1450	1355	3696			
2HB_str_OaHz	2961-3077	1414-1455	1375	3368	1478	1757	1203

^aAtom labels are defined in Figure S.2.1.

^bv($\text{O}_\text{a}\text{H}_\text{z}$) and $\delta_i(\text{O}_\text{a}\text{H}_\text{z})$ are coupled with v(OH_z) and $\delta(\text{OH}_\text{z})$, respectively.

Table S.5.6. Geometrical parameters (pm)^a of BuOHs chemisorbed at the *straight* and *zigzag* channels of H-ZSM-5 obtained using pbcDFT and pbc[DFT-D] approaches.

		H _z --O _a	H--O _b	H _z -O	H-O	q ^b
pbcDFT	<i>Straight channel</i>	1-Butoxonium	152.3	146.0	105.1	107.1
		i-Butoxonium	155.5	148.1	104.2	106.4
		2-Butoxonium	153.1	155.4	105.3	104.7
		t-Butoxonium	164.1	152.7	103.1	105.6
		t-Butoxonium_sym ^c	153.6	157.5	104.8	0.81
pbc[DFT-D]	<i>Zigzag channel</i>	1-Butoxonium	143.8	154.4	107.5	104.7
		1-Butoxonium_sym ^c	149.2	151.3	105.9	105.4
		i-Butoxonium	155.4	144.9	107.1	104.4
		2-Butoxonium	151.2	154.0	105.0	104.6
		t-Butoxonium	155.0	147.1	104.1	106.1
pbc[DFT-D]	<i>Straight channel</i>	1-Butoxonium	153.2	146.7	105.0	106.9
		i-Butoxonium	155.6	147.6	104.2	106.6
		2-Butoxonium	154.3	156.8	104.9	104.5
		t-Butoxonium	164.4	149.0	103.0	106.2
		t-Butoxonium_sym ^c	152.5	157.8	105.1	0.81
pbc[DFT-D]	<i>Zigzag channel</i>	1-Butoxonium	145.5	155.5	107.0	104.4
		1-Butoxonium_sym ^c	149.1	152.5	106.0	105.2
		i-Butoxonium	145.0	155.6	107.1	104.3
		2-Butoxonium	153.0	153.7	104.6	104.8
		t-Butoxonium	155.0	149.7	104.2	105.4

^aAtom labels and chemisorbed notations are defined in Fig. S.3.1. ^bq: formal charge of the protonated butoxonium ($C_4H_9OH_2^+$, R: hydrocarbon chain) chemisorbed in H-ZSM-5. ^cChemisorbed complexes with more symmetric OH covalent bond length.

Table S.5.7. Chemisorption energies (ΔE_{chem} , kJ mol⁻¹) and DFT-D proton transfer energies (ΔE_{pt} , kJ mol⁻¹) of BuOHs at the *straight* and *zigzag* channels of H-ZSM-5 obtained using pbcDFT + D and pbc[DFT-D] approaches.

		ΔE_{chem}				
		$\Delta E_{\text{DFT-D}}$	ΔE_{DFT}	ΔE_{D}	$\Delta E_{\text{pt, DFT-D}}$	
pbcDFT	<i>Straight channel</i>	1-Butoxonium	-152	-86	-66	-2
		i-Butoxonium	-148	-88	-60	+1
		2-Butoxonium	-149	-87	-62	-3
		t-Butoxonium	-151	-87	-64	-1
		t-Butoxonium_sym	-153	-88	-66	-3
pbc[DFT-D]	<i>Zigzag channel</i>	1-Butoxonium	-166	-80	-86	-5
		1-Butoxonium_sym	-166	-80	-86	-5
		i-Butoxonium	-149	-53	-96	+2
		2-Butoxonium	-160	-65	-95	-4
		t-Butoxonium	-149	-46	-103	
pbc[DFT-D]	<i>Straight channel</i>	1-Butoxonium	-150	-84	-66	-2
		i-Butoxonium	-147	-88	-59	0
		2-Butoxonium	-146	-88	-58	-1
		t-Butoxonium	-150	-86	-64	-2
		t-Butoxonium_sym	-151	-88	-63	-3
pbc[DFT-D]	<i>Zigzag channel</i>	1-Butoxonium	-164	-79	-85	-4
		1-Butoxonium_sym	-163	-81	-82	-3
		i-Butoxonium	-146	-51	-95	+1
		2-Butoxonium	-157	-61	-96	-2
		t-Butoxonium	-148	-45	-103	

Table S.5.8. Selected harmonic vibration frequencies (cm^{-1})^a for chemisorbed complexes of BuOHs in H-ZSM-5 obtained using pbcDFT and pbc[DFT-D] approaches. v: stretching mode, δ : bending mode, v_s : symmetric stretching mode, v_a : asymmetric stretching mode.

		v(CH)	$\delta(\text{CH})$	$\delta(\text{CH}_3)$	$v_s(\text{HOHz})$	$v_a(\text{HOHz})$	$\delta(\text{HOHz})$
<i>pbcDFT</i>	1-Butoxonium_zig	2980-3089	1434-1454	1366	2637	2190	1631
	1-Butoxonium_zig_sym	2983-3084	1433-1460	1365	2593	2316	1634
	t-Butoxonium_str	2993-3085	1421-1466	1385	2801	2408	1619
	t-Butoxonium_str_sym	2989-3083	1421-1469	1385	2715	2460	1626
<i>pbc[DFT-D]</i>	1-Butoxonium_zig	2965-3082	1423-1452	1357	2669	2243	1642
	1-Butoxonium_zig_sym	2967-3080	1423-1452	1356	2603	2319	1643
	iso-Butoxonium_str	2947-3060	1419-1447	1373	2666	2292	1628
	2-Butoxonium_zig	2985-3086	1420-1444	1358	2671	2459	1634
	t-Butoxonium_str	2966-3068	1413-1456	1377	2812	2325	1626
	t-Butoxonium_str_sym	2964-3068	1413-1457	1375	2711	2434	1635

^aAtom labels are defined in Figure S.3.1.

S.6. Gas phase proton affinities (PA) of butanols computed using Gaussian at the CBS-QB3 level of theory.

Accurate PAs of butanols are not amenable to direct experimental measurements because of their tendency to form protonated clusters, $(\text{BuOH})_n\text{H}^+$, and/or to dissociate into the alkyl ion plus water.¹ In the more recent NIST compilation by Hunter and Lias,² relative PAs of butanols at 298 K are reported to increase in the order: n-butanol (-789.2 kJ/mol) < i-BuOH (-793.7 kJ/mol) < t-BuOH (-802.6 kJ/mol) < 2-BuOH (-815 kJ/mol), which were evaluated based on the estimation of methyl or alkyl substitution effects on experimentally available references.^{3,4,5} However, Benoit and Harrison⁶ employed a linear relationship between experimentally measured PAs and the ionization energy (IE) for the 1s electron of the oxygen atom of numerous bases and estimated that: n-BuOH (-788 kJ/mol) < 2-BuOH (-791 kJ/mol) < t-BuOH (-810 kJ/mol) in agreement with the trend for PAs of butanols reported by Bomse and Beauchamp.⁷

Due to the discrepancy among evaluated PA data for butanols,¹⁻⁷ the high level of theory CBS-QB3 in Gaussian was therefore used in this study to calculate proton affinities at 0 K of the four

BuOH isomers: 1-BuOH(-834 kJ/mol) < i-BuOH (-836 kJ/mol) < 2-BuOH (-849 kJ/mol) < t-BuOH (-860 kJ/mol) (Table 1). A thermodynamic correction from 0 K to 298 K lowers the PAs of butanols: 1-BuOH (-797 kJ mol^{-1}) \approx i-BuOH (-797 kJ mol^{-1}) < 2-BuOH (-811 kJ mol^{-1}) < t-BuOH (-825 kJ mol^{-1}), in agreement by magnitude with the data reported by Hunter and Lias² and Benoit and Harrison.⁶

Table S.6.1. CBS-QB3 PAs (kJ/mol) vs. NIST PAs (kJ/mol)

	NIST ^a (298 K)	PA-IE ^b (298 K)	CBS-QB3 (0 K)	CBS-QB3 (298 K)
1-BuOH	-789.2	-788	-834	-797
i-BuOH	-793.7	NA	-836	-797
2-BuOH	-802.6	-791	-849	-811
t-BuOH	-815.0	-810	-860	-825

^aThe NIST compilation data for PAs of butanols is taken from ref. 2. ^bThe PAs estimated based on the correlation PA-IE are taken from ref. 6

S.7. Harmonic motions of physisorbed and chemisorbed complexes of butanols in H-ZSM-5

S.7.1. Harmonic motions of physisorbed complexes

Pbc[DFT-D] selected harmonic frequencies of the unloaded H-ZSM-5, gas-phase butanols and the most stable physisorbed states for each of the four butanols are presented in Table S.5.5. Unloaded H-ZSM-5 and all physisorbed complexes have no imaginary frequency and can thus be identified as local minima over the potential energy surface. Harmonic vibrations of unloaded H-ZSM-5 are characterized by the $\nu(\text{O}_\text{a}\text{H}_\text{z})$ stretching at 3737 cm^{-1} together with the in-plane (δ_i) and out-of-plane (δ_o) $\text{O}_\text{a}-\text{H}_\text{z}$ bending at 1110 cm^{-1} and 353 cm^{-1} , respectively. These results are virtually identical to previous pbcDFT calculations (3744 , 1112 and 351 cm^{-1})⁸ and in agreement with MP2 calculations for T-3 clusters (3717 , 1047 and 322 cm^{-1})⁹ as well as the experimental IR-spectrum of H-ZSM-5 (3610 , 1090 , and 320 - 420 cm^{-1}).¹⁰

The IR spectra of the gas phase butanols possess $\nu(\text{CH})$ stretching (2882 - 3056 cm^{-1}) and $\delta(\text{CH})$ bending (1405 - 1464 cm^{-1}), $\delta(\text{CH}_\text{3})$ bending (1348 - 1355 cm^{-1}) and $\nu(\text{OH})$ stretching (3696 - 3759 cm^{-1}) vibrations. By hydrogen bonding with the O_b of the BAS, the $\nu(\text{OH})$ is shifted to

lower wave numbers (3368-3497 cm⁻¹) in comparison with 3400-3461 cm⁻¹ for the physisorbed complexes of C1-C4 primary alcohols computed using the pbcDFT level of theory for geometrical optimization.⁸

Possessing largely elongated O_a-H_z bonds and shortened O---H_z HBs, the physisorbed complexes of the butanols are characterized by strongly intermixed O_a-H_z and O---H_z vibrations, demonstrating the partial proton transfer from the zeolite to the alcohol molecule. It is observed that the v(O_aH_z) is coupled with the v(OH_z) and redshifted to very low wave numbers (1370-1478 cm⁻¹) and falls in the v(CH) region (1414-1460 cm⁻¹). In addition, the in-plane and out-of-plane bending modes are blueshifted to higher wave numbers of 1647-1757 and 1171-1203 cm⁻¹, respectively. The redshift of v(O_aH_z) computed for the physisorbed complexes of butanols in this pbc[DFT-D] study (2266-2374 cm⁻¹) is analogous to 2233-2336 cm⁻¹ predicted for those of the primary C1-C4 alcohols using the pbcDFT⁸ but significantly larger than 1159 cm⁻¹ reported for methanol physisorbed species using cluster calculations at the MP2 level of theory.¹¹ It is well-known from literature that DFT methods tend to overestimate hydrogen-bonding interactions, thus resulting in long O_a-H_z bonds and largely redshifted v(O_aH_z) frequencies.^{11,12} Nonetheless, this study clearly confirms the enhancing effect of accounting for the zeolite framework on the proton transfer from the zeolite to the adsorbed bases.^{8,13} First principles MD calculations based on periodic DFT¹⁴⁻¹⁷ also indicate that the zeolite proton strongly fluctuates midway between the zeolite and the alcohol molecule and that coupling of the O_a-H_z and the alcohol motions occurs.

S.7.2. Harmonic motions of chemisorbed complexes

The results of pbc[DFT-D] frequency calculations for the most stable chemisorbed complexes are reported in Table S.5.8. For all butanols, v(CH), δ(CH) and δ(CH₃) of the oxonium ions are predicted in the region of 2947-3086, 1413-1457, and 1356-1377 cm⁻¹, respectively. These frequencies are essentially identical with those of the physisorbed complexes as well as with those of the gas-phase alcohols. The largely unaffected v(CH) upon adsorption of alcohols in zeolites was also observed in previous theoretical calculations⁸ and experimental studies.¹⁸⁻²²

Three characteristic vibrations, i.e. the δ(H_zOH) (1626-1642 cm⁻¹), the v_s(H_zOH) (2603-2812 cm⁻¹) and the v_a(H_zOH) (2243-2459 cm⁻¹), are observed for all the chemisorbed complexes. It has been mentioned above that for the oxonium ions the two O-H/O_z-H bonds can stretch to a certain extent without significant changes in energy. However, these variations in geometry may lead to

important changes in vibrational frequencies and could explain the broad nature of the experimentally measured OH stretches.^{8,23} For 1-BuOH, the two chemisorbed complexes of largely identical energy, i.e. 1-butoxonium_zig and 1-butoxonium_zig_sym, are characterized by largely different H_z-O-H stretches (2669 and 2243 vs. 2603 and 2319 cm⁻¹). Analogous results are also found for t-butoxonomium_str and t-butoxonomium_str_sym (2812 and 2325 vs. 2711 and 2434 cm⁻¹). These findings suggest that the broad and shallow potential energy surface for H-O and H_z-O bond fluctuation may account for the uncertainties in the H_z-O-H stretching frequencies of alcohol-zeolite complexes.

References

- (1) Holmes, J. L.; Aubry, C.; Mayer, P. M. *J. Phys. Chem. A* **1999**, 103, 705-709.
- (2) Hunter, E.; Lias, S. *J. Phys. Chem. Ref. Data* **1998**, 27, 413-656.
- (3) Pau, J. K.; Kim, J. K.; Caserio, M. C. *J. Am. Chem. Soc.* **1978**, 100, 3831-3837.
- (4) Wolf, J. F.; Staley, R. H.; Taagepera, M.; McIver, R. T.; Beauchamp, Jr. J. L.; Taft, R. W. *J. Am. Chem. Soc.* **1977**, 99, 5417-5429.
- (5) Taft, R. W. et al. *J. Am. Chem. Soc.* **1978**, 100, 7765-7767.
- (6) Benoit, F. M.; Harrison, A. G. *J. Am. Chem. Soc.* **1977**, 99, 3980-3984.
- (7) Bomse D. S.; Beauchamp, J. L. *J. Phys. Chem.* **1981**, 85, 488-492.
- (8) Nguyen, C. M.; Reyniers, M. F.; Marin, G. B. *Phys. Chem. Chem. Phys.* **2010**, 12, 9481-9493.
- (9) Krossner, M.; Sauer, J. *J. Phys. Chem.* **1996**, 100, 6199-6211.
- (10) Mirth, G.; Lercher, J. A.; Anderson, M. W.; Kinowski, J. *J. Chem. Soc., Faraday Trans. 1990*, 86, 3039-3044.
- (11) Haase, F.; Sauer, J. *J. Am. Chem. Soc.* **1995**, 117, 3780-3789.
- (12) Sauer, J.; Ugliengo, P.; Garrone, E.; Saunders, V. R. *Chem. Rev.* **1994**, 94, 2095-2160.
- (13) Greatbanks, S. P.; Hillier, I. H.; Burton, N. A. *J. Chem. Phys.* **1996**, 105, 3770-3776.
- (14) Haase, F.; Sauer, J.; Hutter, J. *Chem. Phys. Lett.* **1997**, 266, 397-402.
- (15) Stich, I.; Gale, J. D.; Terakura, K.; Payne, M. C. *Chem. Phys. Lett.* **1998**, 283, 402-408.
- (16) Haase, F.; Sauer, J. *Microporous Mesoporous Mater.* **2000**, 35-36, 379-385.
- (17) Stich, I.; Gale, J. D.; Terakura, K.; Payne, M. C. *J. Am. Chem. Soc.* **1999**, 121, 3292-3302.
- (18) Makarova, M. A.; Paukshtis, E. A.; Thomas, J. M.; Williams, C.; Zamaraev, K. I. *J. Catal.* **1994**, 149, 36-51.

- (19) Makarova, M. A.; Williams, C.; Zamaraev, K. I. *J. Chem. Soc. Faraday Trans.* **1994**, 90, 2147-2153.
- (20) Makarova, M. A.; Williams, C.; Romannikov, V. N.; Zamaraev, K. I. *J. Chem. Soc. Faraday Trans.* **1990**, 86, 581-584.
- (21) Williams, C.; Makarova, M. A.; Malysheva, L. V.; Paukshtis, E. A.; Zamaraev, K. I. *J. Chem. Soc. Faraday Trans.* **1990**, 86, 3473-3485.
- (22) Williams, C.; Makarova, M. A.; Malysheva, L. V.; Paukshtis, E. A.; Talsi, E. P.; Thomas, J. M.; Zamaraev, K. I. *J. Catal.* **1991**, 127, 377-392.
- (23) Shah, R.; Gale, J. D.; Payne, M. C. *J. Phys. Chem.* **1996**, 100, 11688-11697.